




Excited-state resonance tunneling in strong-field ionizationLijuan Jia , Haijun Xing , and Libin Fu **Graduate School of China Academy of Engineering Physics, No. 10 Xibeiwang East Road, Haidian District, Beijing, 100193, China*

(Received 24 March 2022; accepted 10 August 2022; published 26 August 2022)

We study the tunneling dynamics of a system with two bound states. We find that the system can be effectively described by a two-level leakage cavity model, with which we can reproduce the dynamics of tunneling ionization. It shows that tunneling via the excited-state resonance dominates over the ground-state tunneling within the field strength considered, where the electron prefers jumping to the excited-state resonance channel first and then tunneling out. Moreover, several key parameters of the system naturally emerge in our two-level model. Especially, one of the parameters is the physical correspondence of the tunneling time obtained from the ground-state tunneling.

DOI: [10.1103/PhysRevA.106.022814](https://doi.org/10.1103/PhysRevA.106.022814)**I. INTRODUCTION**

Tunneling ionization is currently referred to as the starting point for essentially most modern strong-field phenomena. Attosecond laser pulses access ultrashort time spans to uncover microscopic details of electron tunneling ionization [1–8]. Electron tunneling has been used in many areas of science and technology, including scanning tunneling microscopy [9], tunnel diodes [10], photosynthesis [11], photoelectron holography [12], laser induced electron diffraction [13,14], and many more.

The earliest theoretical treatments on electron tunneling ionization were based on the strong-field approximation (SFA), known as the Keldysh-Faisal-Reiss (KFR) approach [15–17]. For an approximate analysis of electron tunneling on the subcycle time scale, a convenient closed-form expression for the ionization rate at every moment is derived [18]. Later, a popular three-step semiclassical model [19,20], which can well reproduce the experimental results quantitatively for certain field strength, is developed to analyze the tunneling electron trajectories. Several approaches have also been developed to address electron tunneling ionization [21,22]. For these broadly accepted appealing approaches, however, the dynamics of the tunneling process has not been involved, which is at the heart of understanding many pioneering results in the strong-field tunneling ionization. The most notable is the interpretation of tunneling time defined by the attosecond angular streaking experiments [2,4,5,23–26].

When it turns to studying tunneling dynamics, contributions from the excited states are expected to be non-negligible [27–30]. In fact, excitation of the atom plays an important role in various ionization processes. For instance, resonant enhancement of below-threshold harmonics [31–33], emission from excited states via free induction decay [32,34], high-order harmonic emission through ionization from excited states [34,35]. By amending the KFR theory and comparing

the continuum population with the results of the first principle calculation, the effect of the excited states is evaluated [27]. Meanwhile, the contributions of the excited states often complicate the physical picture of tunneling ionization. Hence, a method of filter function is developed to eliminate the masking signal from excited state [30], with which a tunnel time scaling with the classical Keldysh time [15,36] is defined with a full quantum approach. The Keldysh time is defined as $\tau_k = \sqrt{2I_p}/2F$, where I_p is the electron ionization energy and F is the laser electric field. It measures the time a bound electron with the velocity $v = \sqrt{2I_p}$ takes to cross the tunneling barrier with width $l = I_p/F$.

In this work, we study the tunneling dynamics by solving the Schrödinger equation (SE) without utilizing the filter function. We find that the ionization process, including the contributions of excited states, can be well reproduced by a two-level model of leakage cavity. Each parameter in this model has an explicit physical correspondence, which thus provides a clear picture to show the tunneling process of the electron and the role of excited state in tunneling dynamics. Moreover, each parameter is related to a time scale. Thus, the model suggests a convenient way to quantify the tunneling process. Interestingly, based on the quantified times extracted from our model, we have obtained the physical correspondence of the tunnel time defined in Ref. [30] within the field range in our consideration.

II. TUNNELING THROUGH A BARRIER IN A HOMOGENEOUS FIELD

We consider an electron trapped in a one-dimensional (1D) square-well potential interacting with a static electric field. The electron is initially in its ground state, and the field is applied instantaneously at $t = 0$. Within the dipole approximation and the length gauge, the Hamiltonian is modeled as

$$H = \begin{cases} T + V(x), & \text{for } t < 0, \\ T + V_{\text{eff}}(x), & \text{otherwise,} \end{cases} \quad (1)$$

*lbfu@gcaep.ac.cn

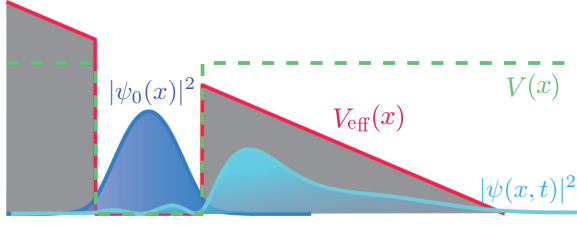


FIG. 1. Field-induced tunneling ionization. The square-well potential $V(x)$ and the effective potential $V_{\text{eff}}(x)$ are shown in dashed green and solid red lines, respectively. $|\psi_0(x)|^2$ (blue) and $|\psi(x,t)|^2$ (cyan) are the distributions of the (initial) ground electron wave function and tunneling wave function.

where T is the kinetic energy, $V(x)$ is the potential with the depth $-V_0$ and the width $2a$, and

$$V_{\text{eff}}(x) = \begin{cases} -V_0, & \text{for } |x| < a, \\ -xF, & \text{otherwise,} \end{cases} \quad (2)$$

F is the static electric field. A plot of the potentials is shown in Fig. 1. A triangular barrier is formed by combining the square-well potential with the static field.

The time-independent Schrödinger equation (TISE) of this field-dressed system is

$$\left(-\frac{1}{2} \frac{\partial^2}{\partial x^2} + V_{\text{eff}}(x) \right) \psi_\varepsilon(x) = \varepsilon \psi_\varepsilon(x), \quad (3)$$

which can be solved analytically [37,38]. ε is the eigenenergy that ranges from $-\infty$ to $+\infty$ and $\psi_\varepsilon(x) = \langle x | \psi_\varepsilon \rangle$ represents its corresponding eigenstate wave function. For $t \geq 0$, time propagation is handled by expanding the wave function of electron $|\psi(t)\rangle$ on the basis of these eigenstates as

$$|\psi(t)\rangle = \sum_j g_0(\varepsilon_j) e^{-i\varepsilon_j t} |\psi_{\varepsilon_j}\rangle, \quad (4)$$

where $g_0(\varepsilon_j) = \langle \psi_{\varepsilon_j} | \psi_0 \rangle$ is the projection coefficient of the unperturbed ground state to eigenstates. Here, we have chosen a discrete notation for the energy ε and the spectral probability amplitude $g_0(\varepsilon)$ of the continuum states consistent with the finite box size used in the numerical simulations.

In this work, we choose $V_0 = 2$ a.u. and $a = 1.5$ a.u.. Under these parameters, the field-free system contains two bound states; that is, a ground state $|\psi_0\rangle$ with eigenenergy $E_0 = -1.696$ a.u. and an excited state $|\psi_1\rangle$ with eigenenergy $E_1 = -0.846$ a.u.. In the numerical calculations, we have used the absorbed boundary condition. The box size is $(-106, 106)$, which is far larger than the range of the initial square-well potential. We have checked the convergence of the results. Atomic units are used throughout the paper unless otherwise noted.

A. Single-mode ground-state tunneling

In the presence of the perturbation, the bound electron would be free from the binding potential by tunneling through the triangular barrier. In this section, We follow the method suggested in Ref. [30] to figure out the tunneling dynamics and obtain the time it takes during this process.

The wave function of electron $|\psi(t)\rangle$ for $t > 0$ can be described as

$$|\psi(t)\rangle = a_0(t)|\psi_0\rangle + |\phi(t)\rangle, \quad (5)$$

where $|\psi_0\rangle$ is the unperturbed ground state and $a_0(t) = \langle \psi_0 | \psi(t) \rangle$. The unnormalized $|\phi(t)\rangle$ is the part of the wave function orthogonal to the ground state; that is, $\langle \psi_0 | \phi(t) \rangle = 0$. Substitute Eq. (5) into the time-dependent Schrödinger equation (TDSE) with the Hamiltonian given in Eq. (1) and multiply both sides by $\langle \psi_0 |$. With assuming $|\phi(t)\rangle = a_0(t)|\varphi(t)\rangle$ and defining $\Delta E_0(t) \equiv \langle \psi_0 | H | \varphi(t) \rangle$, we finally arrive at the expression

$$\Delta E_0(t) = i \frac{\dot{a}_0(t)}{a_0(t)} - E_0, \quad (6)$$

which is the time-dependent generalization of Fano resonance theory [39]. It determines a finite spectral width of the field-free ground state. By using the expansion in Eq. (4), $\Delta E_0(t)$ can also be recast as

$$\Delta E_0(t) = \frac{\sum_j \varepsilon_j |g_0(\varepsilon_j)|^2 e^{-i\varepsilon_j t}}{\sum_j |g_0(\varepsilon_j)|^2 e^{-i\varepsilon_j t}} - E_0. \quad (7)$$

Introducing

$$w_0(t) \equiv -2 \text{Im}\{\Delta E_0(t)\} = -\partial \log[p_0(t)] / \partial t, \quad (8)$$

it gives the ionization rate at which probability leaves the ground state, and $p_0(t)$ is the population probability of ground state.

Figure 2(b) shows the ionization rate $w_0(t)$ of ground state. It presents strong oscillations for short times, followed by a steady value. To understand the temporal behaviors of $w_0(t)$ in the quantized channel picture [30], the spectral density $|g_0(\varepsilon)|^2$ (solid blue line) as a function of energy ε at $F = 0.6$ a.u. is plotted in Fig. 2(a). The peaks of $|g_0(\varepsilon)|^2$ reveal the spectral signature of the tunnel ionization dynamics. These peaks, from left to right, represent the waves coming from ground-state resonance, the first excited-state resonance, and other continuum resonances. And the width of the peak determines the ionization rate of corresponding resonance channels. For short times, in response to the laser field, the excited-state resonance creates relatively intense outward propagating initial waves, which can jump to the ground state and cause the strong oscillations of $w_0(t)$. For longer times, the signals via excited-state resonance become weak and decay faster than the oscillation period. Thus, the ionization rate $w_0(t)$ reaches a steady value.

Afterwards, to eliminate the signal stemming from the excited-state resonance, a technique of a filter function is employed. In Fig. 2(a), we plot the filtered $|g_0(\varepsilon)|^2$ (dashed red line), which isolates the part of the ground-state wave function escaping via the ground-state resonance. The filter function is set as

$$f(\varepsilon) = \begin{cases} 1 & \text{for } \varepsilon < \varepsilon_c, \\ e^{(\varepsilon - \varepsilon_c)^2 / 2\sigma^2} & \text{for } \varepsilon \geq \varepsilon_c, \end{cases} \quad (9)$$

where ε_c is the central energy of the peak of spectral density and σ is the width (standard deviation) of the filter function. $\sigma = 0.125$ for $F = 0.6$ a.u.. After filtering, the probability current flowing back to the ground state is eliminated. As

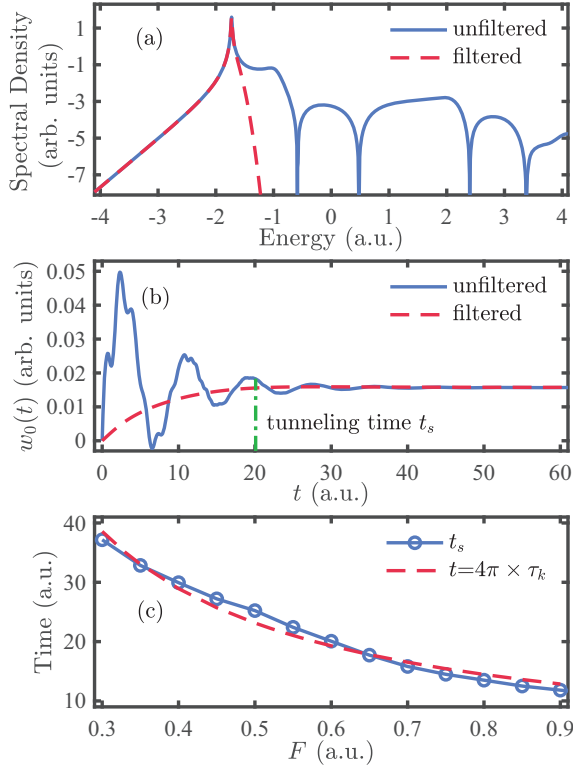


FIG. 2. (a) Spectrum density $|g_0(\varepsilon)|^2$ as a function of energy, ε and (b) ionization rate, $w_0(t)$, for the unfiltered (solid blue line) and filtered (dashed red line) cases. Here $F = 0.6$ a.u. and parameters of the 1D square-well potential are $V_0 = 2$ a.u. and $a = 1.5$ a.u.. (c) Calculated t_s as a function of the field strength, F . For comparison, the Keldysh time τ_k multiplied by 4π is shown as the dashed red line.

a result, the ionization rate $w_0(t)$ of the ground state rises monotonically and approaches a steady-state value, as shown in Fig. 2(b) (dashed red line). We call this tunneling way of ignoring the ground-state dynamics as single-mode ground-state tunneling and define the rise time as the single-mode tunneling time t_s , correspondingly.

The time t_s is determined at which the relative error is 1% of its steady-state value. We give the time t_s for $F = 0.6$ a.u., and marked it by dash-dotted green line in Fig. 2(b). Obviously, a shorter time is needed to approach a steady-state value for the filtered case. Also, we have calculated the time t_s for different field strengths F . As shown in Fig. 2(c), t_s is approximately proportional to the Keldysh time as $t_s \approx 4\pi \times \tau_k$. Different from our case, $t_s \approx 4.4 \times \tau_k$ for the quantum dot and $t_s \approx 5.8 \times \tau_k$ for the 1D model atom, respectively in [30]. We mention that the discrepancy in the proportional coefficient not only depends on the initial state, determined by the shape of the trap potential, but also relates to the temporal evolution of the wave function, which is significantly affected by the shape of the barrier potential [38].

As stated above, the tunneling time t_s only represents the time it takes to establish a steady probability flow from the ground state. It can only characterize the partial ground-state tunneling dynamics. With considering the contribution of the excited states, what will be the physical correspondence

of t_s in the whole tunneling dynamics? This will be explained in detail in the following sections.

B. Tunneling described by a model of leakage cavity

Let us go back to the starting point of the tunneling event of a bound electron. In this section, we generalize Eq. (5) to multiple bound states, where the temporal wave function $|\psi(t)\rangle$ can be written in the form

$$|\psi(t)\rangle = \sum_i a_i(t)|\psi_i\rangle + |\phi(t)\rangle, \quad (10)$$

where $|\psi_i\rangle$ ($i = 0, 1, 2, \dots$) is the i th unperturbed bound state and $a_i(t) = \langle\psi_i|\psi(t)\rangle$ is the probability amplitude, correspondingly. The unnormalized $|\phi(t)\rangle$ is the part of the wave function ionized from the potential and is orthogonal to the bound states; that is, $\langle\psi_i|\phi(t)\rangle = 0$ for all i . Inserting Eq. (10) into TDSE and projecting over the subspace $\langle\psi_i|$, we have a differential equation for $a_i(t)$

$$i\dot{a}_i(t) = E_i a_i(t) + \langle\psi_i|H_0 - Fx|\phi'(t)\rangle, \quad (11)$$

with $E_i = \langle\psi_i|H_0|\psi_i\rangle$, and $|\phi'(t)\rangle = \sum_{j \neq i} a_j|\psi_j\rangle + |\phi(t)\rangle$, contains all the states that can jump to the i th bound state. Denoting $|\phi'(t)\rangle = a_i(t)|\varphi(t)\rangle$, we arrive at the expression

$$\Delta E_i(t) = i \frac{\dot{a}_i(t)}{a_i(t)} - E_i, \quad (12)$$

with $\Delta E_i(t) \equiv \langle\psi_i|H|\varphi(t)\rangle$; $w_i(t) = -2 \text{Im}\{\Delta E_i(t)\} = -\partial \log[p_i(t)]/\partial t$ gives the rate at which probability leaves the i th bound state and escapes to other bound states or continuums. When $i = 0$, it turns out to be Eq. (8). Accordingly, the ionization rate $w(t)$ at which probability leaves the trap potential rather than the ground state and escapes into the continuum is

$$w(t) = -\frac{\partial \log[p(t)]}{\partial t} = -\frac{\dot{p}(t)}{p(t)}, \quad (13)$$

where $p(t) = \sum_i p_i(t)$ is the total probability of the unperturbed bound states.

From the expansion Eq. (4), it is straightforward to rewrite the expression for ionization rate $w(t)$ as

$$w(t) = \frac{\sum_{ij} i(\varepsilon_i - \varepsilon_j) e^{-i(\varepsilon_i - \varepsilon_j)t} G_{ij}}{\sum_{ij} e^{-i(\varepsilon_i - \varepsilon_j)t} G_{ij}}, \quad (14)$$

where $G_{ij} = |g_{0i}|^2 |g_{0j}|^2 + \sum_{e=1}^N g_{0i} g_{0j}^* g_{ei}^* g_{ej}$, g_{0i} is short for $g_0(\varepsilon_i)$, $g_{ei} \equiv g_e(\varepsilon_i) = \langle\psi_{\varepsilon_i}|\psi_e\rangle$ is the spectral amplitude of the e th unperturbed excited state, and N is the number of the unperturbed excited states. In our current considered system, it contains two bound states, i.e., $N = 1$.

Equation (14) incorporates information of the spectra of ground state and excited state, as depicted in Fig. 3(a). To show the contribution of the excited state, with the same parameters, we plot the ionization rate of the ground state $w_0(t)$ for the unfiltered case and ionization rate $w(t)$ at $F = 0.6$ a.u. in Fig. 3(b). It shows that $w_0(t)$ and $w(t)$ are different quantitatively in many characteristics, which include the amplitude, the damping rate, the oscillation period, and the time at which a steady value is achieved. Besides, a time delay exists between $w_0(t)$ and $w(t)$. These all imply that the excited

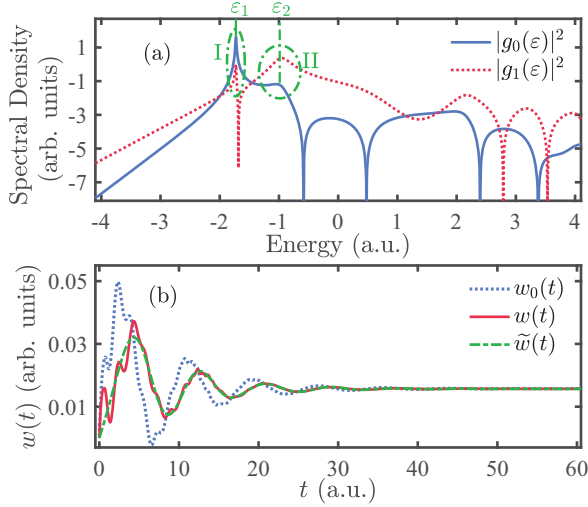


FIG. 3. (a) Spectrum densities $|g_0(\varepsilon)|^2$ (solid blue line) and $|g_1(\varepsilon)|^2$ (dotted red line) as a function of energy. The first peak and second peak of the spectra are marked by I and II, respectively. ε_1 and ε_2 are the corresponding central energies. (b) The ionization rate of ground state $w_0(t)$ (dotted blue line) and the ionization rate $w(t)$ (solid red line). The ionization rate $\tilde{w}(t)$ (dash-dotted green line) is the result of the four peaks marked by I and II. Here, $F = 0.60$ a.u.

state plays a non-negligible role in the process of tunneling ionization. We also find that the ionization dynamics can be well presented by selecting only the first two peaks [marked by I and II in Fig. 3(a)] of the spectra, whose central energies are ε_1 and ε_2 , respectively. The resulting $\tilde{w}(t)$ of the four peaks is shown in Fig. 3(b). Except for the rapid oscillations for shorter times, $\tilde{w}(t)$ shows in good agreement with $w(t)$. This finding is accessible for all other field strengths investigated.

Besides, for different field strengths, the ionization rate $w(t)$ displays a similar behavior, as shown in Figs. 4(a)–4(d) (solid blue lines). They all initially present a strong but damped oscillation and finally reach a steady value. A tunneling time τ_w can be extracted from this crossover, at which the relative error of the ionization rate to its steady value is 1%. Therefore, without considering the rapid oscillations for shorter times and based on the dissipation and oscillation

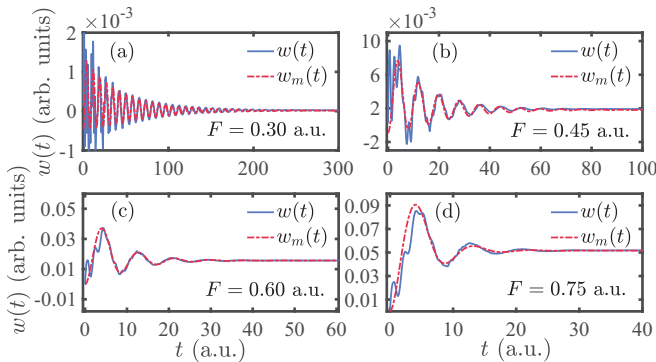


FIG. 4. (a)–(d) The ionization rate $w(t)$ (solid blue lines) and the fitted $w_m(t)$ (dash-dotted red lines) for field strength $F = 0.30, 0.45, 0.60, 0.75$ a.u., respectively.

behaviors of $w(t)$, we try to introduce a simple two-level model of leakage cavity to characterize the dynamics of tunneling process intuitively. The non-Hermitian Hamiltonian of a typical leakage cavity can be represented as [40,41]

$$H_m = \begin{pmatrix} E_1 - i\Gamma_1/2 & V \\ V & E_2 - i\Gamma_2/2 \end{pmatrix}. \quad (15)$$

We identify E_1 and E_2 as the two binds of the bound stable energy states. Γ_1 (Γ_2) determines the leakage rate from the lower (higher) energy channel E_1 (E_2). V is the interaction. Together with Γ_1 and Γ_2 , it determines the survival time of particles in this model.

Denoting $c_1(t)$ and $c_2(t)$ as the time-dependent probability amplitudes of the two states in the model, they satisfy the equations

$$\begin{aligned} i\dot{c}_1(t) &= (E_1 - i\Gamma_1/2)c_1(t) + Vc_2(t), \\ i\dot{c}_2(t) &= Vc_1(t) + (E_2 - i\Gamma_2/2)c_2(t). \end{aligned} \quad (16)$$

In analogy to the tunneling event of a bound electron and Eq. (13), we have the leakage rate $w_m(t)$ of this model

$$w_m(t) = -\frac{\partial_t(|c_1(t)|^2 + |c_2(t)|^2)}{|c_1(t)|^2 + |c_2(t)|^2}. \quad (17)$$

With assuming $E_2 > E_1$ and $\Gamma_2 > \Gamma_1$ in our considered case, the Eq. (17) for longer times becomes

$$w_m(t \rightarrow \infty) = \text{Im}[\Omega] + \frac{\Gamma_1 + \Gamma_2}{2}, \quad (18)$$

with $\Omega = \sqrt{\Delta E^2 + 4V^2}$ and $\Delta E = E_2 - E_1 - i(\Gamma_2 - \Gamma_1)/2$. This implies that the asymptotic value of the ionization rate relates to all parameters. The set of parameters (δE , Γ_1 , Γ_2 , V) involved in the leakage process are obtained by fitting $w_m(t)$ with $w(t)$.

Figure 4 shows the fitting results $w_m(t)$ (dash-dotted red lines) for a wide range of field strengths. Surprisingly, we find that the fitting results well coincide with the original data for long times. Since the long-time behavior of $w(t)$ largely comes from the contributions of the sharp peaks of the spectra [42], as $\tilde{w}(t)$ shows. Hence, this leakage model can be used to reproduce the process of tunneling ionization.

III. REVEALING AND QUANTIFYING THE TUNNELING PROCESS

Since the parameters in the leakage model have their own physical meaning and characterize the leakage behaviors of particles, we can reveal the dynamics of electron tunneling based on these parameters of this model. We numerically fit the set of parameters (δE , Γ_1 , Γ_2 , V) for different external laser strengths F . The result is plotted in Fig. 5(a). It shows that Γ_2 drastically increases with increasing F . Γ_1 is about three orders of magnitude smaller than Γ_2 . This implies that the leakage channel of the lower state is nearly turned off. And, the interaction V , by which the particles can be transported from the lower state to the higher state, is approximately proportional to the field strength F . Specifically, we have $V \approx 0.35 \times F \langle \psi_0 | x | \psi_1 \rangle$, which shows a tight connection between V and the transition element of two bound states.

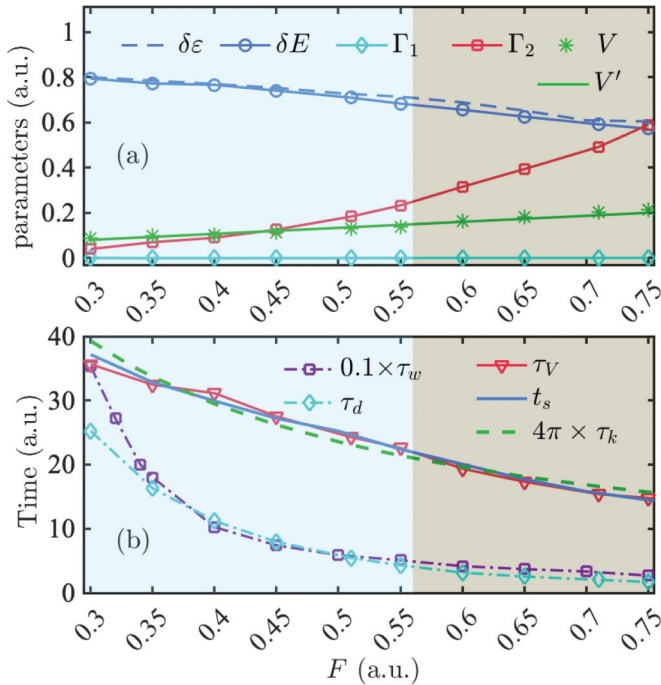


FIG. 5. (a) Parameters (δE , Γ_1 , Γ_2 , V) as a function of field strength F . The energy gap $\delta\varepsilon = \varepsilon_2 - \varepsilon_1$, and $V' = 0.35 \times F \langle \psi_0 | x | \psi_1 \rangle$. (b) Kinds of typical times as functions of field strength F . The blue region ($F \leq 0.56$ a.u.) and gray region ($F > 0.56$ a.u.) represent the first excited state being bound and unbound, respectively.

Note that the external laser field turns discrete bound states into mixed bound-continuum resonance states with a finite spectral width. In Fig. 3(a), the sharp peak marked by I represents tunnel ionization via the ground-state resonance, and the broad peak marked by II corresponds to ionization via the excited-state resonance. From the result of $\tilde{w}(t)$ [dash-dotted green line in Fig. 3(b)], the long-time behavior of $w(t)$ is thus captured by the interference between the outward propagating waves coming from the resonance channels of ground state and excited state. Interestingly and importantly, as shown in Fig. 5(a), δE is approximately equal to the central energy gap $\delta\varepsilon$ ($\delta\varepsilon = \varepsilon_2 - \varepsilon_1$) of the two peaks of spectra. This approximate agreement reveals a notable physical correspondence that the two levels of the leakage model roughly correspond to the resonance channels of ground state and excited state.

This roughly physical correspondence suggests an explicit picture of the ionization dynamics in the tunneling process based on the behaviors of the set of parameters (δE , Γ_1 , Γ_2 , V) in the model. Initially, an electron populates at the ground state. Switching on the external field, the electron tunnels out of the barrier via the two resonance channels. The electron probes a potential barrier of larger height and width in the ground state, it thus prefers to tunnel in two steps: first, it leaves the ground state and jumps to the resonance channel of excited state; second, it tunnels out by this excited-state channel, within the field strength we consider. From this tunneling picture, the time delay between the first oscillation peaks of $w_0(t)$ and $w(t)$ [see Fig. 3(b)] becomes clear. The first peak of $w_0(t)$ is formed by the first step. While, that of $w(t)$ is mainly

contributed by these two combined processes, and the second step takes time generally.

Furthermore, every parameter in this model is related to a time scale. Due to the good reproducibility of the model, the tunneling process can be quantified via these parameters.

We obtain kinds of typical times, as presented in Fig. 5(b). The tunneling time τ_w is the response time it takes the part of the wave function tunneling from the barrier to establish a steady ionization rate. The damping time $\tau_d = 1/\Gamma_2$ characterizes the interference time of the initial waves coming from the resonance tunneling channels of ground state and excited state. It determines the damping period of the ionization rate $w(t)$. As expected, the behaviors of τ_w and τ_d changing with the external field F are the same qualitatively. As the field strength F increases, smaller width and lower height of the barrier are formed. This yields that the initial waves from the excited-state ionization channel pass beyond the bound region more quickly, resulting in the descent of τ_w and τ_d .

We define an interaction time as $\tau_V = \pi/V$. V determines the speed of transporting the electron from the ground state to the excited state. To figure out more clear physics involved in the single-mode ground-state tunneling, the single-mode tunneling time t_s is again plotted in Fig. 5(b). Interestingly, we find that it is nearly identical to the time τ_V . Hence, we take τ_V as the correspondence of t_s within the field strength we considered. It indicates that the single-mode ground-state tunneling only characterizes one step, the electron leaves the ground state, in the whole tunneling ionization process. In general cases, leaving the ground state is not equivalent to tunneling out of the barrier, since the second step of our tunneling picture is also time consuming. As a result, without utilizing a filter function, we present the main results in Ref. [30] and also emphasize the non-negligible role of the excited state playing in tunneling dynamics.

In addition, the field is separated into two regions in Fig. 5. For $F \leq 0.56$ a.u., the excited state is bound. Otherwise, it is over the barrier. We can see that regardless of the excited state being bound or unbound, the fitting parameters and the typical times change smoothly with increasing the field strength. Besides, the ionization rates $w(t)$ for $F > 0.56$ a.u. display the same temporal behaviors as $F \leq 0.56$ a.u., as shown in Fig. 4. These indicate that it seems unnecessary to distinguish between tunneling and over-the-barrier ionizations in the study of tunneling dynamics. Similar findings have been presented in Ref. [38].

IV. CONCLUSIONS

In conclusion, the introduced two-level model of leakage cavity has well reproduced the tunneling ionization of a bound electron and presented a clear picture of electron tunneling, among which the excited-state resonance tunneling can dominate over the ground-state resonance tunneling. Based on this model, the single-mode ground-state tunneling, suggested in Ref. [30] is only an indispensable step in the tunneling process within the field strength range in our study.

In this case of static field, the electron finds a more efficacious tunneling way; that is, tunneling occurs readily from the resonance channels. An analogous and attractive tunneling pathway has also been excavated when the atom is subject

to a time-varying field whose frequency is not resonant with transition to an eigenstate [43]. The smart electron will first gain energy by virtual absorption of photons to reach virtual off-the-energy-shell states and then tunnel from them efficiently.

In this current studied system, which contains two field-free bound states, two dominated resonance channels have been obtained. If, within a range of field intensities, the ground-state resonance and the excited-state resonance always play a major role in the tunneling dynamics regardless of the number of unperturbed bound states, the generalization of our model to a multilevel system may be achieved. We also hope that we can generalize the current methods to more realistic potentials (for instance, Coulomb potential) in a full-dimensional system by using a time-varying field. Moreover,

an exponential decay in time corresponds to a Lorentzian spectrum. From the view of Lorentzian spectrum, one may construct a more general model to reproduce the predictions of Schrödinger equation. This may suggest another convenient way to help us reveal more physical details involved in the tunneling dynamics of an electron.

ACKNOWLEDGMENTS

L.J. appreciates many useful discussions with Dr. L. Xu, Dr. J. Chen, and Dr. F. Deng. This work was supported by the National Natural Science Foundation of China (Grants No. 11725417, No. 12088101, No. 12047548, and No. U1930403), and Science Challenge Project (Grant No. TZ2018005).

-
- [1] P. Eckle, M. Smolarski, P. Schlup, J. Biegert, A. Staudte, M. Schöffler, H. G. Muller, R. Dörner, and U. Keller, *Nature Phys.* **4**, 565 (2008).
- [2] P. Eckle, A. N. Pfeiffer, C. Cirelli, A. Staudte, R. Dörner, H. G. Muller, M. Büttiker, and U. Keller, *Science* **322**, 1525 (2008).
- [3] U. S. Sainadh, R. T. Sang, and I. V. Litvinyuk, *J. Phys. Photon.* **2**, 042002 (2020).
- [4] U. S. Sainadh, H. Xu, X. Wang, A. Atia-Tul-Noor, W. C. Wallace, N. Douguet, A. Bray, I. Ivanov, K. Bartschat, A. Kheifets, R. T. Sang, and I. V. Litvinyuk, *Nature (London)* **568**, 75 (2019).
- [5] L. Torlina, F. Morales, J. Kaushal, I. Ivanov, A. Kheifets, A. Zielinski, A. Scrinzi, H. G. Muller, S. Sukiasyan, M. Ivanov, and O. Smirnova, *Nature Phys.* **11**, 503 (2015).
- [6] C. Hofmann, A. S. Landsman, and U. Keller, *J. Mod. Opt.* **66**, 1052 (2019).
- [7] U. Saalman and J. M. Rost, *Phys. Rev. Lett.* **125**, 113202 (2020).
- [8] A. S. Landsman, M. Weger, J. Maurer, R. Boge, A. Ludwig, S. Heuser, C. Cirelli, L. Gallmann, and U. Keller, *Optica* **1**, 343 (2014).
- [9] G. Binnig, H. Rohrer, C. Gerber, and E. Weibel, *Phys. Rev. Lett.* **49**, 57 (1982).
- [10] L. Esaki, *Phys. Rev.* **109**, 603 (1958).
- [11] E. Drigo Filho, K. H. P. Jubilato, and R. M. Ricotta, *Braz. J. Phys.* **50**, 575 (2020).
- [12] Y. Huismans, *Science* **331**, 61 (2011).
- [13] M. Meckel, D. Comtois, D. Zeidler, A. Staudte, D. Pavicic, H. C. Bandulet, H. Pepin, J. C. Kieffer, R. Dörner, D. M. Villeneuve, and P. B. Corkum, *Science* **320**, 1478 (2008).
- [14] C. I. Blaga, J. Xu, A. D. Dichiaro, E. Sistrunk, K. Zhang, P. Agostini, T. A. Miller, L. F. Dimauro, and C. D. Lin, *Nature (London)* **483**, 194 (2012).
- [15] L. V. Keldysh, *Sov. Phys. JETP* **20**, 1307 (1965).
- [16] F. H. M. Faisal, *J. Phys. B* **6**, L89 (1973).
- [17] H. R. Reiss, *Phys. Rev. A* **22**, 1786 (1980).
- [18] M.V. Ammosov, D.B. Delone, and V.P. Krainov, *Sov. Phys. JETP* **64**, 1191 (1986).
- [19] P. B. Corkum, *Phys. Rev. Lett.* **71**, 1994 (1993).
- [20] M. Lewenstein, P. Balcou, M. Y. Ivanov, A. L'Huillier, and P. B. Corkum, *Phys. Rev. A* **49**, 2117 (1994).
- [21] G. L. Yudin and M. Y. Ivanov, *Phys. Rev. A* **64**, 013409 (2001).
- [22] S. V. Popruzhenko, *J. Phys. B: At. Mol. Opt. Phys.* **47**, 204001 (2014).
- [23] I. A. Ivanov and A. S. Kheifets, *Phys. Rev. A* **89**, 021402(R) (2014).
- [24] H. Ni, U. Saalman, and J.-M. Rost, *Phys. Rev. A* **97**, 013426 (2018).
- [25] H. Ni, U. Saalman, and J.-M. Rost, *Phys. Rev. Lett.* **117**, 023002 (2016).
- [26] J. M. Rost and U. Saalman, *Nature Photon.* **13**, 439 (2019).
- [27] E. E. Serebryannikov and A. M. Zheltikov, *Phys. Rev. Lett.* **116**, 123901 (2016).
- [28] T. Debnath, M. S. B. M. Yusof, P. J. Low, and Z.-H. Loh, *Nature Commun.* **10**, 2944 (2019).
- [29] O. Smirnova, M. Spanner, and M. Ivanov, *J. Phys. B: At. Mol. Opt. Phys.* **39**, S307 (2006).
- [30] C. R. McDonald, G. Orlando, G. Vampa, and T. Brabec, *Phys. Rev. Lett.* **111**, 090405 (2013).
- [31] M. Chini, X. Wang, Y. Cheng, H. Wang, Y. Wu, E. Cunningham, P. C. Li, J. Heslar, D. A. Telnov, S. I. Chu, and Z. Chang, *Nature Photon.* **8**, 437 (2014).
- [32] S. Camp, K. J. Schafer, and M. B. Gaarde, *Phys. Rev. A* **92**, 013404 (2015).
- [33] E. S. Toma, P. Antoine, A. de Bohan, and H. G. Muller, *J. Phys. B: At. Mol. Opt. Phys.* **32**, 5843 (1999).
- [34] S. Beaulieu, S. Camp, D. Descamps, A. Comby, V. Wanie, S. Petit, F. Légaré, K. J. Schafer, M. B. Gaarde, F. Catoire, and Y. Mairesse, *Phys. Rev. Lett.* **117**, 203001 (2016).
- [35] X.-B. Bian and A. D. Bandrauk, *Phys. Rev. Lett.* **105**, 093903 (2010).
- [36] A. S. Landsman and U. Keller, *Phys. Rep.* **547**, 1 (2015).
- [37] L. D. Landau and E. M. Lifshitz, *Quantum Mechanics: Non-Relativistic Theory* (Pergamon, New York, 1991).
- [38] L. Jia, L. Xu, P. Zhang, and L. Fu, *New J. Phys.* **23**, 113047 (2021).
- [39] U. Fano, *Phys. Rev.* **124**, 1866 (1961).
- [40] M. Grisaru, H. Pendleton, and R. Petrasso, *Ann. Phys. (NY)* **79**, 518 (1973).
- [41] P. R. Fontana and D. J. Lynch, *Phys. Rev. A* **2**, 347 (1970).
- [42] J.-B. Yuan, H.-J. Xing, L.-M. Kuang, and S. Yi, *Phys. Rev. A* **95**, 033610 (2017).
- [43] M. Klaiber and J. S. Briggs, *Phys. Rev. A* **94**, 053405 (2016).